

# Neuromorphic Encoding / Decoding of Data-Event Streams Based on the Poisson Point Process Model

Viacheslav Antsiperov<sup>a</sup>

*Kotelnikov Institute of Radioengineering and Electronics of RAS, Mokhovaya 11-7, Moscow, 125009, Russia*

**Keywords:** Neuromorphic Computing, Data-Event Streams, Poisson Counts, Sampling Representation, Receptive Fields, Most Powerful Unbiased Test, Center / Surround Inhibition, Perceptual Coding, Marr's Image Primal Sketch.

**Abstract:** The work is devoted to a new approach to neuromorphic encoding of streaming data. An essential starting point of the proposed approach is a special (sampling) representation of input data in the form of a stream of discrete events (counts), modeling the firing events of biological neurons. Considering the specifics of the sampling representation, we have formed a generative model for the primary processing of the count stream. That model was also motivated by known neurophysiological facts about the structure of receptive fields of sensory systems of living organisms that implement universal mechanisms (including central-circumferential inhibition) of biological neural networks, particularly the brain. To list the main ideas and consolidate the notations used, the article provides a brief overview of the features and most essential provisions of the proposed approach. The new results obtained within the framework of the approach, related to the analysis of neuromorphic encoding (with distortions) of streaming data, are discussed. The issues of possible decoding/restoration of the original data are discussed in the context of what Marr called the primary sketch. The results of computer modelling of the developed encoding/decoding procedures are presented, approximate numerical characteristics of their quality are given.


## 1 INTRODUCTION

The widespread use of computers in (Big) data processing tasks has shifted the focus from issues of fitting data to known statistical models to issues of developing adequate (generative) models based on the characteristics of the data themselves. The most successful here have been artificial neural networks (ANN), capable of automatically (machine-aided) learning on data without explicit additional programming of the systems. Since the effectiveness of machine learning (ML) depends primarily on the volume of data, very high requirements for performance, available resources, and the data exchange capacity of computers are important here. The rapidly developing technologies of deep learning (DL) are the most critical to such requirements (Dargan, 2020). It is deep learning that has enabled the development of more efficient, intelligent and scalable solutions for many information tasks over the past decades, including recognition and synthesis of text, speech, images, as well as for such real-world

tasks as market segmentation, customer consulting, self-driving cars, etc.

Unfortunately, today we understand that the progress achieved in the field of information technology, due to successes in the development of the element base of computers, will not be able to continue forever. The main problem here is that existing computers are oriented towards the von Neumann architecture. The latter assumes a continuous, intensive exchange of information between the memory and the processor via a common bus. The presence in modern computers of a limited bus bandwidth, due to fundamentally physical (thermodynamic) principles, will eventually lead to a slowdown in the progress observed today. Neither Moore's doubling law nor Dennard's scaling law will save us from the inevitable crisis.

A promising direction for solving this problem seems to be the transition to neuromorphic computing based on several neurobiological principles of the human brain (Christensen, 2022). A typical information technology that can make maximum use

<sup>a</sup> <https://orcid.org/0000-0002-6770-1317>

of the advantages of neuromorphic data processing are systems for controlling and monitoring objects based on a stream of recorded images. In this regard, we note such a new area of information technology as neuromorphic vision (NV) (Wang, 2023). NV involves recording images using neuromorphic cameras and processing them using spiking neural networks (SNNs). The difference between NV and traditional computer vision lies primarily in the way of image formation by the data registered. Traditional computer vision involves the accumulation of data over a certain registration time frame, treating the result of the accumulation as an image. Neuromorphic vision, in contrast, is focused on presenting data in the form of a continuous stream of discrete events (counts), recorded by neuromorphic cameras (Al-Obaidi, 2021). Accordingly, calculations in NV must necessarily be neuromorphic – event-driven, as, for example, in SNN networks.

Thus, neuromorphic technologies open new horizons that allow us not only to focus on digital computing, but also to rethink the use of analog, approximate and mixed data computing, typical for biological neurons. At the same time, neuromorphic computing will require a radical change in the programming paradigm. This may be why neuromorphic computing has yet to find widespread market adoption – to date, there are only a few publicly discussed prototypes, the result of initiatives from a few leading universities and academic centres.

With this in mind, we have recently attempted to develop some methods for processing data streams based on procedures that would be based on the neuromorphic-like computing (Antsiperov V., 2024). An essential starting point is a special (sampling) representation of input data in the form of a stream of discrete events (counts), like firing events of biological receptors. Considering the specifics of the sampling representation, we have formed a generative model based on known neurophysiological facts about the system of receptive fields (RF) of the living sensory systems, which implement universal mechanisms (including center-surround inhibition) of the biological neural networks. To recall the main ideas and to fix the notations used, the next section provides a short review of the features and most essential provisions of the approach. The following sections discuss new results related to the analysis of neuromorphic coding of data and the formation on its basis of what Marr called a primary sketch (Marr, 1980), i.e. a procedure of neuromorphic data primary reconstruction. We note in this regard that Marr's concept of a primary sketch is today considered as a first step towards Gestalt synthesis (Zhu, 2023).

## 2 MAIN FEATURES OF NEUROMORPHIC COMPUTING BASED ON A POISSON STREAMS OF DISCRETE EVENTS

Let's start the discussion with the main provisions of the approach we are developing to neuromorphic computing. Since our approach was largely formed on the way of modeling neural structure and functions of sensory systems of living organisms, the architecture and concepts of neuromorphic systems used in the approach are discussed in terminology like that used in neurobiology. Terms and concepts from the neurophysiology of the most complex and universal sensory system, the human visual system (HVS), are widely used. Due to the known similarity of the neuro-mechanisms of most biological sensory systems (touch, hearing, vision or smell) (Masland, 2020), the HVS terminology can be well adapted to each of them and can also be successfully used in the case of artificial neuromorphic systems that model biological.

As noted above, a feature of approach proposed is its special form of input data representation. Our approach doesn't assume input data in traditional form of a continuous distribution of stimuli intensity  $I(\vec{x})$  over a certain parametric space  $\vec{x} \in \Omega \subset R^d$  – in the case of HVS – the intensity of the incident on the retina  $\Omega \subset R^2$  radiation, but in the form of a stream of random, discrete events  $X = \{\vec{x}_i\}$ ,  $\vec{x}_i \in \Omega$  that result from the process of detecting such intensity – in the case of HVS by retinal receptors depolarizations – the so-called (photo) counts. The process of registering random events itself is assumed to be as simple as possible: the probability of registering an event in a small element of the parametric space  $d\vec{x} \in \Omega$  is assumed to be proportional to the power of the recorded data:  $P(\vec{x}_i) \sim I(\vec{x}_i)d\vec{x}$ ; the probability of registering two or more events in the same element  $d\vec{x}$  is considered negligible in comparison with  $P(\vec{x}_i)$ ; and events in separated elements are considered as statistically independent (dependent only on  $I(\vec{x})$ ). It is known that the listed properties (orderliness and independence) are “almost necessary” for the corresponding event stream to be a  $d$  –dimensional inhomogeneous Poisson point process (PPP) (Kingman, 1993) with a point-count rate  $\lambda(\vec{x})$  proportional to the intensity  $I(\vec{x})$ . A detailed discussion of numerous issues, approximations and applications of PPP to the event stream modeling can be also found in the books (Streit, 2010) and (Barrett,

2004). A statistical description of such a representation can also be obtained using the concepts of an *ideal recording device* and an *ideal image*, proposed in our work (Antsiperov, 2023).

From the statistical point of view, the representation of the event stream  $= \{\vec{x}_i\}$ ,  $i = 1, \dots, n$ , by PPP implies the identification of registered event parameters  $\vec{x}_i$  with the PPP random point having the same coordinates in the same parameter space  $\Omega \subset R^d$ . Accordingly, a complete statistical description of the events could be given by the joint distribution density of PPP points. Here, however, it should be noted, that the number of points in PPP is potentially infinite, but the number  $n$  of actually recorded events is always finite. To get around this problem, for a given region  $\Omega$ , one can specify the (consistent) set of joint finite-dimensional distributions for all  $n = 0, 1, \dots$ . Such description of events is traditionally called as the *preset-time* form (Barrett, 2004). But one can fix  $n$  and consider the representation  $X_n = \{\vec{x}_i\} \subset X$  as a subsample of size  $n$  from the general population of all PPP points. This description is called the *preset-counts* form (Barrett, 2004). The latter representation was used in most of our works and was defined as a *sampling representation* (Antsiperov, 2023). Under the assumption of independence of counts, the sampling representation joint probability distribution density decomposes into the product of individual count densities:  $\rho_n(X = \{\vec{x}_i\} | I(\vec{x})) = \prod_{i=1}^n \rho_1(\vec{x}_i | I(\vec{x}))$ , where the density of the individual count  $\rho_1(\vec{x}_i | I(\vec{x}))$  coincides with the normalized (to region  $\Omega$ ) intensity (Antsiperov, 2023):

$$\rho_1(\vec{x}_i | I(\vec{x})) = \frac{I(\vec{x}_i)}{\int_{\Omega} I(\vec{x}) d\vec{x}}. \quad (1)$$

Note that the given description of the event stream (1) is very convenient for both theoretical analysis and numerical simulation. Indeed, factorization of the joint distribution density into the product of individual count densities  $\rho_1(\vec{x}_i | I(\vec{x}))$  is the basis for many well-developed statistical approaches and is assumed by a few ML methods, including naive Bayes learning (Murphy, 2012). Namely, if the intensity  $I(\vec{x})$  is known at least approximately, it is possible using (1) to carry out complex calculations with  $\rho_n(X = \{\vec{x}_i\} | I(\vec{x}))$  basing on the Monte Carlo methods (Robert, 2004).

To illustrate this thesis, Figure 1 shows the result of count stream modelling for the intensity  $I(\vec{x})$  specified by the pixels of the PNG image “GRAY\_OR\_400x400\_056.png” of size  $s \times s = 400 \times 400$  pixels, color depth  $v = 8$  bits from the TESTIMAGES database (Asuni, 2014). The set  $X_n = \{\vec{x}_i\}$  of  $n = 10\,000\,000$  random counts was

generated by the Monte-Carlo acceptance-rejection sampling method (Robert, 2004) with a uniform auxiliary distribution  $u(\vec{x}) = s^{-2}$  and an auxiliary constant  $M = 2^v$ , details can be found, for example, in (Antsiperov, 2023).

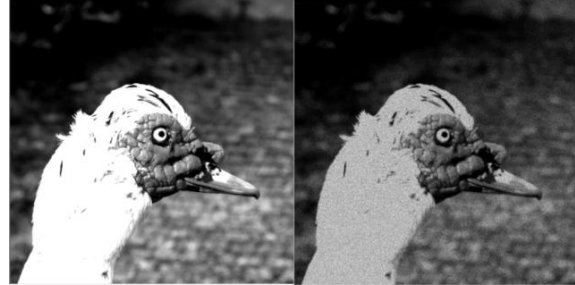


Figure 1: Illustration of event stream represented by Poisson counts (sampling representation), generated by Monte Carlo acceptance-rejection sampling. On the left side is the approximate intensity  $I(\vec{x})$  given by the pixels in the grayscale image “GRAY\_OR\_400x400\_056.png” (Asuni, 2014). On the right – its sampling representation of size  $n = 10\,000\,000$  counts.

The advantage of event stream description in the form (1) is also its universal character, allowing to transition from detailed (ideal) fine-scale consideration at the level of individual events (points) to a more coarse, large-scale analysis in the form of the number of events in any area  $\sigma \subset \Omega$  of parametric space. A similar transformation occurs in the retina of the eye, which contains  $\sim 10^8$  receptors (rods and cones), transmitting registered data to the visual cortex only through  $\sim 10^6$  axons of output neurons (RGCs - retinal ganglion cells) constituting the optic nerve (Frisby, 2010). As a result, the average ratio of the number of receptors to nerve fibers is about 100:1, which approximately corresponds to the compression of recorded data by interneurons in intermediate layers of the retina. Moreover, it is well known that compression by interneurons (horizontal, amacrine and other cells) is carried out by summing and aggregating the counts of special groups of receptors, that make up the receptive fields (RF) of the corresponding RGCs (Masland, 2020). Since we will need this aggregated representation of event streams below, let's briefly look at how it is derived from the sampling representation (1). Let us denote by  $\Delta \subset \Omega$  a small region in parametric space. The probability that some event  $\vec{x}_i$  from  $X$  will be in  $\Delta$  can be calculated according (1) as:

$$P_1(\Delta) = \int_{\Delta} \rho_1(\vec{x}_i | I(\vec{x})) d\vec{x}_i = \frac{\int_{\Delta} I(\vec{x}_i) d\vec{x}_i}{\int_{\Omega} I(\vec{x}) d\vec{x}}. \quad (2)$$

Accordingly, the probability that some  $k$  of  $n$  (independent) events from  $X = \{\vec{x}_i\}$  will fall into  $\Delta$  is

determined by the binomial distribution  $B(n, P_1(\Delta))$ , for which we immediately write out the asymptotic for large  $n \gg k$ :

$$\begin{aligned} P_k(\Delta) &= \frac{n!}{k!(n-k)!} P_1^k(\Delta) (1 - P_1(\Delta))^{n-k} = \\ &= \frac{(nP_1(\Delta))^k}{k!} \frac{\prod_{i=1}^{n-k} (1 - \frac{i}{n})}{(1 - P_1(\Delta))^k} \left(1 - \frac{nP_1(\Delta)}{n}\right)^n \rightarrow \cdot, \quad (3) \\ &\rightarrow \frac{(\beta \bar{I}(\Delta) \sigma)^k}{k!} \exp(-\beta \bar{I}(\Delta) \sigma) \end{aligned}$$

where it is assumed that together with  $n \rightarrow \infty$  also  $\iint_{\Omega} I(\vec{x}) d\vec{x} \rightarrow \infty$ , so that  $\iint_{\Omega} I(\vec{x}) d\vec{x} / n \sim \beta^{-1} = \text{const}$ , from which it follows that  $\beta^{-1}$  is the portion of the total power of the recorded  $I(\vec{x})$  per count. The symbol  $\sigma$  in (3) denotes the area of the region  $\Delta$ , the value  $\bar{I}(\Delta) = \iint_{\Delta} I(\vec{x}_i) d\vec{x}_i / \sigma$  denotes the average intensity  $I(\vec{x})$  on  $\Delta$ , thus  $nP_1(\Delta) \sim \beta \iint_{\Delta} I(\vec{x}_i) d\vec{x}_i = \beta \bar{I}(\Delta) \sigma$ . As a result, the probability distribution of the number of events (3) turns out to be Poisson (similar to the preset-time representation, but on  $\Delta$ , not on  $\Omega$ ), for which the average  $k$  (as well as its variance) is equal to  $\bar{k} = \beta \bar{I}(\Delta) \sigma$ . Distribution (3) does not depend on the details of  $I(\vec{x})$  on  $\Delta$ , but only on the average integral characteristic  $\bar{I}(\Delta)$ , which, in fact, implies a coarsening of the description. To simplify the notation, it is advisable to introduce instead of  $\bar{I}(\Delta)$  a proportional measure of the average number of events  $\lambda(\Delta) = \bar{k} = \beta \bar{I}(\Delta) \sigma$ , which completely determines the distribution of events number  $k$  on  $\Delta$ . Note that  $k$ , in turn, is an unbiased estimate of  $\lambda(\Delta)$  (with the minimum possible variance which is equal to the reciprocal of the Fisher information in  $k$ ).

The derivation of distribution (3) can be easily extended to  $m > 1$  disjoint regions  $\Delta_j \in \Omega$ ,  $j = 1, \dots, m$ , with the numbers of events  $\{k_j\}$ . As a result, the set  $Y = \{k_j\}$  will be a collection of independent Poisson random variables with a joint distribution (in asymptotic  $k = \sum_{j=0}^m k_j \ll n \rightarrow \infty$ ) of the form:

$$\begin{aligned} P_m(Y = \{k_j\} | I(\vec{x})) &= \\ &= \prod_{j=1}^m \frac{(\lambda(\Delta_j))^{k_j}}{k_j!} \exp(-\lambda(\Delta_j)). \end{aligned} \quad (4)$$

In the case when the union of similar disjoint areas  $\{\Delta_j\}$  covers a significant part of the event stream area  $\Omega$  (i.e., it partitions the latter), the set  $Y = \{k_j\}$  together with its statistical description (4) can be considered as coarsened (to a scale of  $\sim \sigma$ ) stream representation. In (Antsiperov, 2023) it was called the “*occupation-number*” representation. The occupation number representation (4) is related to the sampling representation (1) in the same way as in statistical physics the canonical ensemble is related to the microcanonical one.

As noted above, the numbers  $k_j$  can be interpreted as unbiased estimates of the means  $\bar{k}_j = \beta \iint_{\Delta_j} I(\vec{x}) d\vec{x}$ . If we assume that all regions  $\Delta_j$ , located in different places of  $\Omega$ , are similar to each other in shape (the shape of a typical region  $\Delta$ ), then  $\{\bar{k}_j\}$  will be the output of a linear filter with a sliding window  $\Delta$  from the input  $I(\vec{x})$ . Moving average filters are well known in computer science and are a classic tool for simple denoising (encoding) of signals of various origins. In this sense, the representation  $Y = \{k_j\}$  does not contain anything fundamentally new and is widespread with the only note that its noise is assumed not to be additive Gaussian, but Poissonian (or quantum noise, or shot noise (Barrett, 2004)). To illustrate such a representation (by occupancy numbers) Figure 2 shows the representation  $Y = \{k_j\}$  for rectangular lattice of  $50 \times 50$  regions over the  $\Omega$ .

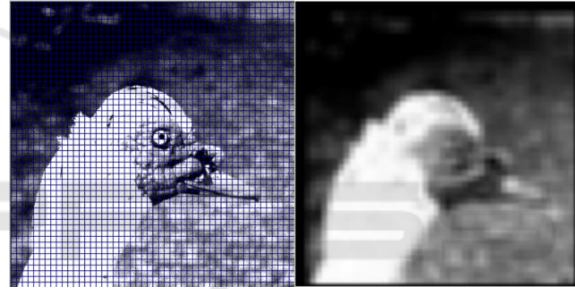


Figure 2: Image sampling representation coarsened by the rectangular lattice. On the left is a sampling representation of size 10 000 000 counts of the grayscale image from Figure 1, covered with a  $50 \times 50$  lattice. On the right – smoothed coarsened representation  $Y = \{k_j\}$ , obtained by a rectangular lattice of  $50 \times 50$  square regions.

### 3 POISSON STREAMS NEUROMORPHIC ENCODING BY THE SYSTEM OF THE RECEPTIVE FIELDS

Unfortunately, the above simple occupancy number representation  $Y = \{k_j\}$ , along with the advantage of simplicity of encoding ( $400 \times 400$  pixels  $\rightarrow$   $50 \times 50$  matrix), has a number of significant disadvantages. This problem is well known in the field of image coding (Zhang, 2021). The problem is that moving average filters are low-pass filters and, therefore, while eliminating the redundancy associated with uncorrelated noise, they also suppress significant fine details in data. The latter leads to blurring of contrasts,

destruction of boundaries, smoothing of important texture fragments., etc., i.e. all those characteristics that are extremely important for a human when analyzing the data (Masland, 2020). Moreover, linear filters are no longer effective at suppressing noise in cases where the latter depends on the signal, as in the case of Poisson noise. To combat these circumstances, various nonlinear modifications of filters have been proposed, in particular, based on anisotropic filtering, total variation, SUSAN filter, empirical Wiener filter, thresholding wavelet-shrinkage, bilateral filter, mean-shift filter, etc., see (Buades, 2005). Many of these nonlinear filters solve some specific problems of linear processing, but none of them have proven to be universal. Thus the natural guiding principle for the search for universal solutions became the study and modeling of the biological sensory systems neuromechanisms, that possess the required universality. As result, the new direction of research and development of coding / filtering methods focused on human perception has emerged (Antsiperov V. E., 2024).

Most coding methods aimed at human perception are based on the Retinex concept (Land, 1971), which allows separating the reflective radiation from objects from the smoothly changing general illumination of the scene by highlighting or even enhancing the local contrast of image intensity. Among the algorithms based on Retinex, the widely used principle is center/surround inhibition (Jobson, 1997). It estimates a smoothed version of the image (illuminance) and subtracts it from the original image to produce reflectance. Some center/surround algorithms differ in the types of filters that are used to smooth the image. So, SSR (Single Scale Retinex) and MSR (Multi Scale Retinex) algorithms use a Gaussian filter / set of filters. Further development of these ideas led to the creation of a bilateral filter, whose weighting coefficients are a combination of both the spatial proximity of the pixels and the similarity of their values (Elad, 2005). Practice has confirmed that the bilateral filter under smooth lighting well preserves edges and avoids the appearance of associated halos.

The successes of the perceptual coding reflect successful solutions in modeling the internal structure of disjoint areas  $\{\Delta_j\}$  covering (partitioning) the event stream area  $\Omega$ , and on the base of which the occupation number representation  $Y = \{k_j\}$  (4) is constructed. Such centre–antagonistically structured areas are called retinal receptive fields (RF) (Lisani, 2020). Quite unexpected is the fact that the relatively simple organization of the RF in the form of center/surround structure allows, among other things,

to transmit significant information about intensity contrasts to the brain (Masland, 2001).

The lateral inhibition associated with RFs become today the canon of ideas about the basic neurophysiological mechanisms of the perceptual coding. We owe these discoveries primarily to the famous Harvard School, led by Kuffler (Katz, 1982). According to Kuffler the structure of the RF consists of two concentric parts: a central region that receives data directly from the retinal receptors and called the RF center, and an enclosing it (antagonistic) region that receives data from the horizontal cells and called the surround. It is usually believed that the ratio of the center size to the size of the RF (size of the surround) is on average  $\sim 1:2$  (Marr, 1980). Based on the listed neurobiological data, a number of formal models of the center/surround RF have recently been proposed, which, with varying degrees of generality, explain the mechanisms of lateral inhibition using cascades of linear/nonlinear procedures (LN–, LNLN–models) (Zapp, 2022), based on standard elements of ANN. We have also proposed a centre-lateral threshold filtering approach (of NLN type), which was initially focused on processing event streams in neuromorphic systems (Antsiperov V.E., 2024). The features of our approach that distinguish it from those noted above can be found in the article (Antsiperov V., 2024), here we briefly describe only its main points.

Let us denote for some typical RF  $\Delta \subset \Omega$  of area  $\sigma$  by  $\Delta_c$  the region of its center of area  $\sigma_c$  and, accordingly, by  $\Delta_s$  the concentric surround of area  $\sigma_s$ . Assuming that the center and surround do not intersect  $\Delta_c \cap \Delta_s = \emptyset$  and  $\Delta = \Delta_c \cup \Delta_s$ , we say, that  $\Delta_c$  and  $\Delta_s$  perform a partition of RF  $\Delta$ . Note, that in this case  $\sigma = \sigma_c + \sigma_s$ . Let us also denote by  $k$ ,  $k_c$  and  $k_s$  the count numbers in RF  $\Delta$ , in its centre  $\Delta_c$  and surround  $\Delta_s$ :  $k = k_c + k_s$ . As discussed above, these random numbers have Poisson statistical models with probability distributions following from (3):

$$\begin{aligned} k_c \sim P_{k_c}(\Delta_c) &= \frac{(\lambda(\Delta_c))^{k_c}}{k_c!} \exp(-\lambda(\Delta_c)), \\ k_s \sim P_{k_s}(\Delta_s) &= \frac{(\lambda(\Delta_s))^{k_s}}{k_s!} \exp(-\lambda(\Delta_s)), \end{aligned} \quad (5)$$

Since  $k_c$  and  $k_s$  correspond to non-intersecting regions  $\Delta_c \cap \Delta_s = \emptyset$ , they are statistically independent, and their joint distribution can be written, according (5), as:

$$\begin{aligned} P_{k_c, k_s}(\Delta_c, \Delta_s) &= P_{k_c}(\Delta_c) \times P_{k_s}(\Delta_s) = \\ &= \frac{(\lambda(\Delta_c))^{k_c}}{k_c!} \frac{(\lambda(\Delta_s))^{k_s}}{k_s!} \exp\{-\lambda(\Delta_c) + \lambda(\Delta_s)\}. \end{aligned} \quad (6)$$

In order to obtain some conclusions about the behaviour of the intensity  $I(\vec{x})$  in the RF region  $\Delta$ , basing only on the recorded numbers  $k$ ,  $k_c$  and  $k_s$ , regardless of the directly unobservable measures

$\lambda(\Delta_c) = \beta \bar{I}(\Delta_c) \sigma_c$  and  $\lambda(\Delta_s) = \beta \bar{I}(\Delta_s) \sigma_s$  it is necessary to move from conditional distributions (6) (for given  $\lambda(\Delta_c)$  and  $\lambda(\Delta_s)$ ) to unconditional distributions of observable  $k_c$  and  $k_s$ . Adhering to the Bayesian point of view, this can be done by choosing a certain prior distribution for  $\lambda(\Delta_c)$  and  $\lambda(\Delta_s)$ , forming on this basis a generative model of all data  $\{k_c, k_s, \lambda(\Delta_c), \lambda(\Delta_s)\}$  and obtaining from their joint distribution marginal distributions for recorded numbers. We carry out this plan for two different hypotheses: hypothesis  $H_0$ , which assumes the hard dependence of the average intensities  $\bar{I}(\Delta_c)$  and  $\bar{I}(\Delta_s)$  and alternative  $H_1$ , which assumes that  $\bar{I}(\Delta_c)$  and  $\bar{I}(\Delta_s)$  are independent. Obviously,  $H_0$  corresponds to the absence of contrast  $I(\vec{x})$  on  $\Delta$ , and  $H_1$  makes the contrast expectable.

Let the *a priori* distribution of the average intensity  $\bar{I}$  in any region of  $\Omega$  be given by the density  $\rho_a(\bar{I})$  so, that  $\bar{I}$  is not dependent on which RF region  $\Delta_c$ ,  $\Delta_s$  or  $\Delta$  the averaging occurs over. Then, for hypotheses  $H_0$  and  $H_1$  we can write the following forms of their joint distributions:

$$\begin{aligned}
 \rho_a(\bar{I}(\Delta_c), \bar{I}(\Delta_s) | H_i) &= \rho_i(\bar{I}(\Delta_c) | \bar{I}(\Delta_s)) \rho_a(\bar{I}(\Delta_s)), \\
 \rho_0(\bar{I}(\Delta_c) | \bar{I}(\Delta_s)) &= \delta(\bar{I}(\Delta_c) - \bar{I}(\Delta_s)), \\
 \rho_1(\bar{I}(\Delta_c) | \bar{I}(\Delta_s)) &= \rho_a(\bar{I}(\Delta_c)) \rho_a(\bar{I}(\Delta_s)).
 \end{aligned} \quad (7)$$

where  $\delta()$  is Dirac's delta-function,  $i = 0, 1$ .

Multiplying (6) and (7) we obtain the joint distributions of all observable / hidden data  $\{k_c, k_s, \lambda(\Delta_c), \lambda(\Delta_s)\}$  (generative model), integrating them over  $\lambda(\Delta_c)$ ,  $\lambda(\Delta_s)$  we obtain unconditional distributions of observables  $k_c, k_s$  under the assumptions of hypothesis  $H_0$  or its alternative  $H_1$  –  $P_0(k_c, k_s)$  and  $P_1(k_c, k_s)$ . Taking the ratio of these distributions, we obtain the classical likelihood ratio  $\Lambda_{k_c, k_s}$  of the hypothesis  $H_0$  to the alternative  $H_1$ . Skipping a number of transformations and simplifications (details can be found in (Antsiperov V., 2024)), we present bellow only the final, easily interpreted expression for the likelihood ratio:

$$\Lambda_{\delta, k} \approx \frac{k_a}{\sqrt{2\pi k}} \sqrt{\frac{\sigma_c \sigma_s}{\sigma^2}} \exp\left(-\frac{\sigma^2}{2k\sigma_c\sigma_s} \delta^2\right), \quad (8)$$

where  $k = k_c + k_s$ ,  $\delta = k_c - (\sigma_c/\sigma)k$  and  $\bar{k}_a = \beta \bar{I}_a \sigma$  is *a priori* average number of counts on typical RF,  $\bar{I}_a$  is *a priori* average intensity in any region of  $\Omega$  – characteristic scale of *a priori* density  $\rho_a(\bar{I}) \sim \bar{I}_a^{-1}$ .

Using the uniformly most powerful unbiased (UMP) test (Young, 2005), we can now compare the goodness of fit of hypotheses  $H_0$  and  $H_1$  to the available data  $\delta, k$ . Namely, according to the Neyman–Pearson criterion we should accept  $H_0$  – hypothesis of the coincidence  $\bar{I}(\Delta_c) = \bar{I}(\Delta_s)$  if  $\Lambda_{\delta, k} > K_\alpha$  and reject  $H_0$ , implying  $H_1$  – hypothesis of

the existing difference between  $\bar{I}(\Delta_c)$  and  $\bar{I}(\Delta_s)$ , in opposite case  $\Lambda_{\delta, k} < K_\alpha$ . The positive constant  $K_\alpha$  used here depends on the value of  $\alpha$  – the size of the test. The size of the test, in turn, can be defined as the probability of falling data  $\delta, k$  into the critical region  $C_\alpha = \{\delta, k | \Lambda_{\delta, k} < K_\alpha\}$  :  $\alpha = \sum_{\delta, k \in C_\alpha} P_0(\delta, k)$ . From (8) we can obtain the explicit form of  $C_\alpha$ :

$$\frac{\sigma^2}{2k\sigma_c\sigma_s} \delta^2 > \ln \left\{ \frac{k_a}{\sqrt{2\pi k}} \sqrt{\frac{\sigma_c \sigma_s}{\sigma^2}} \frac{1}{K_\alpha} \right\} = d_\alpha^2, \quad (9)$$

from where we can relate the threshold  $d_\alpha$  to the test size  $\alpha$ :

$$\alpha = \frac{2}{\sqrt{\pi}} \int_{d_\alpha}^{\infty} \exp\{-\xi^2\} d\xi = \text{erfc}(d_\alpha), \quad (10)$$

where  $\text{erfc}(x) = \frac{2}{\sqrt{\pi}} \int_x^{\infty} \exp\{-\xi^2\} d\xi$  is standard complementary error function. Thus there is no need to obtain  $d_\alpha$  via the constant  $K_\alpha$  if  $\alpha$  is given. In accordance with (10),  $d_\alpha$  is equal to  $\alpha$ -th quantile of error function  $\text{erfc}(x)$ , which is well tabulated. After  $d_\alpha$  is fixed, the criterion for rejecting the hypothesis  $H_0$  – the hypothesis of the coincidence  $\bar{I}(\Delta_c) = \bar{I}(\Delta_s)$  and assumptions about a possible jump in intensity  $I(\vec{x})$ , contrast on  $\Delta$  takes the following final form:

$$|\delta| > \sqrt{2 \frac{\sigma_c \sigma_s}{\sigma^2}} k d_\alpha. \quad (11)$$

An important conclusion follows from the above discussion: if the “occupancy number” representation code  $Y = \{k_j\}$  is supplemented with the “contrast fields” data, for which residual  $|\delta_j|$  exceeds the threshold specified on the right side of (11), then the resulting code  $Z = \{k_j, \delta_j\}$  will have significantly higher quality, at least in the perceptual sense (for more detailed analysis see (Antsiperov V., 2024)). Figure 3 demonstrates the code  $Z = \{k_j, \delta_j\}$  for the same sampling representation partitioned by the lattice of  $50 \times 50$  square RFs as in Figure 2.

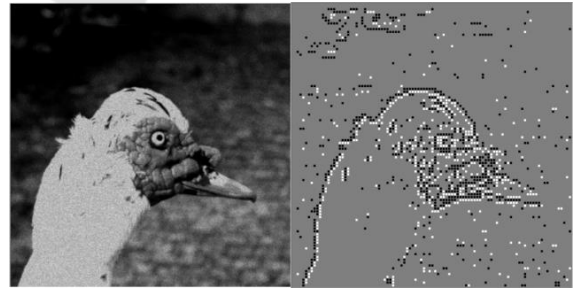


Figure 3: Illustration of the encoding results  $Z = \{k_j, \delta_j\}$  on a rectangular lattice of  $50 \times 50$  RFs for a sampling representation of size 10 000 000 counts from Figures 1, 2. On the left is the sampling representation (Figure 1, right), on the right are RFs with notable values  $\delta_j$ :  $\delta_j > \sqrt{2k}$  in white,  $\delta_j < \sqrt{2k}$  in black ( $\sqrt{\sigma_c \sigma_s / \sigma^2} d_\alpha$  is equal to unity).

## 4 DECODING POISSON STREAMS ENCODED BY THE RECEPTIVE FIELDS SYSTEM

As can be seen from Figure 3, the coding procedure (11) outlines the contrast edges in the image with two chains of non-zero RFs – one chain with positive values  $\delta_j > \sqrt{2k \sigma_c \sigma_s} / \sigma d_\alpha$ , and the other with negative values  $\delta_j < -\sqrt{2k \sigma_c \sigma_s} / \sigma$ . This fact is not accidental. In reality, there is a very close connection (see (Antsiperov V., 2024)) between the values of  $\delta_j$  and the Laplacian of Gaussian (LoG) filter output, which Marr proposed to detect the edges in digital images (Marr, 1980). Namely, to detect the points of such edges – filter zero-crossings, Map proposed to analyze pairs of points with the maximum and minimum of LoG output values, which, as he supposed, correspond to pairs of neighboring RFs with positive and negative responses. Moreover, Marr associated such points with ON- and OFF- receptive fields, as was done from the very beginning in our approach.

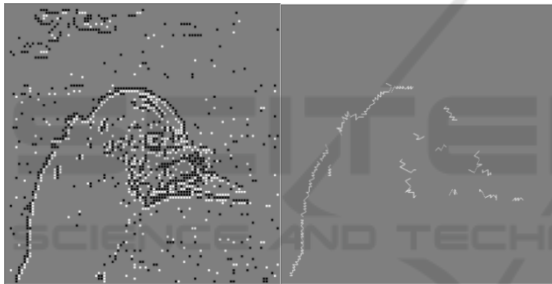


Figure 4: Results of constructing chains of ON- and OFF-field pairs based on  $Z = \{k_j, \delta_j\}$  code for sampling representation of size 10 000 000 counts from Figures 1, 2. On the left is the sampling representation (Figure 1, right), on the right corresponding chains of ON- and OFF-field pairs, obtained by analysis areas with size of  $5 \times 5$  RFs.

Thus, following Marr's concept (Marr, 1980), it is possible to develop procedure for reconstructing (decoding) poisson streams by restoring, in addition to the smoothed intensity, also the edges of contrasts, as discussed above. In fact, the difficult part of this problem is to develop such sub procedure, that selects from the set of all RFs those chains of pairs of ON- and OFF- fields that actually follow along some zero-crossing lines and reject those non-zero  $\delta_j$  RFs that are caused by the random fluctuations and do not determine zero-crossing lines (see Fig. 3 (right)). If this problem is solved and, in addition, the order of the fields in the selected chains is found (see Fig. 4 right), then there are many ways to smoothly interpolate such broken zigzag-shaped sequences with smooth

contours, for example, using Bezier curves (De Boor, 1978), B-splines (Grove, 2011), Laplace smoothing of chains (Vollmer, 1999), etc (see Fig. 5 right).

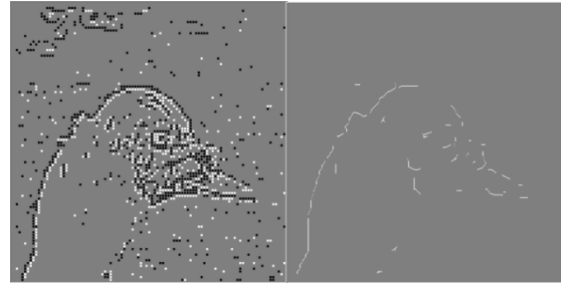


Figure 5: Results of chains smoothing, for sampling representation of size 10 000 000 counts from Figures 1, 2. On the left is the sampling representation (Figure 1, right), on the right Laplace smoothed chain. Note: chains shorter than three segments were censored.

## 5 CONCLUSIONS

As follows from the above, the work proposes a new approach to the problems of neuromorphic coding of data-event streams. Within the framework of the proposed approach, it was possible to carry out explicit modeling of the mechanisms of primary neuro-processing of video data in the periphery of the visual system. As a result, it was possible to develop a constructive method of neuromorphic type of event streams coding. Moreover, the experience of numerical testing and optimization of the developed procedures (algorithms) has shown that based on the concept central to the proposed approach – sampling representations – it is possible, on the one hand, to avoid computational problems associated with processing massive data, and, on the other hand, to adapt the approach to modern neural network problems like the one considered.

In terms of technical implementation, a feature of the proposed method is the widespread use of the neurobiological concept of receptive fields. Structuring data based on a system of receptive fields allows one to effectively circumvent the known difficulties of many numerical algorithms (for example, EM) that process mixtures with many components. This conclusion follows, among other things, from the existing experience in computer implementation of the method. All illustrative materials presented in the work were obtained as part of computational experiments. Experiments confirmed the effectiveness of the method in terms of memory resources/computation time.

In general, based on the results obtained, the

author expresses the hope that the approach proposed in the work and the procedures developed will find both their further theoretical development and fruitful use in applied problems.

## REFERENCES

- Al-Obaidi, S., Al-Khafaji, H. and Abhayaratne C. (2021). Making sense of neuromorphic event data for human action recognition. In *IEEE Access*, V. 9, P. 82686–82700. doi: 10.1109/ACCESS.2021.3085708.
- Amri, E., Felk, Y., Stucki, D., Ma, J., Fossum, E. (2016). Quantum Random Number Generation Using a Quanta Image Sensor. In *Sensors*, V. 16(7), P. 1002. doi: 10.3390/s16071002.
- Antsiperov, V. (2023). New Centre/Surround Retinex-like Method for Low-Count Image Reconstruction. In *Proceedings of the 12th International Conference on Pattern Recognition Applications and Methods (ICPRAM 2023)*, SCITEPRESS, P. 517–528. doi: 10.5220/0011792800003411
- Antsiperov, V. (2024). Neuromorphic Encoding / Reconstruction of Images Represented by Poisson Counts. In *Proceedings of the 13th International Conference on Pattern Recognition Applications and Methods (ICPRAM 2024)*, SCITEPRESS, P. 485–493. doi: 10.5220/0012574100003654.
- Antsiperov, V. E. (2024). Adaptive Filtering of Distributed Data Based on Modeling the Perception Mechanisms of Living Sensory Systems. In: *Vlachos, D. (ed) Mathematical Modeling in Physical Sciences. ICMSQUARE 2023. Springer Proceedings in Mathematics & Statistics*, V. 446, P. 19–31. doi: 10.1007/978-3-031-52965-8\_2
- Asuni, N., Giachetti, A. (2014). TESTIMAGES: a large-scale archive for testing visual devices and basic image processing algorithms. In: *STAG: Smart Tools & Apps for Graphics*, A. Giachetti (Editor).
- Barrett, H. H. and Myers, K. J. (2004). *Foundations of Image Science*, John Wiley and Sons, Hoboken.
- Buades, A., Coll, B., Morel, J. M. A. (2005). Review of Image Denoising Algorithms, with a New One. *Multiscale Modeling & Simulation*, V. 4(2), P. 490–530. Doi: 10.1137/040616024.
- Christensen, D.V., et al. (2022). 2022 roadmap on neuromorphic computing and engineering. In *Neuromorph. Comput. Eng.*, V. 2, P. 022501 doi: 10.1088/2634-4386/ac4a83.
- Dargan, S., Kumar, M., Ayyagari, M. R. et al. (2020) A Survey of Deep Learning and Its Applications: A New Paradigm to Machine Learning. In *Archives of Comput. Methods in Eng.*, V. 27, P. 1071–1092. <https://doi.org/10.1007/s11831-019-09344-w>.
- De Boor, C. (1978) A practical guide to splines. Springer-Verlag, New York; Berlin.
- Elad, M. (2005) Retinex by Two Bilateral Filters. In *Lecture notes in computer science*, Springer, Berlin, Heidelberg, P. 217–229. doi: 10.1007/11408031-19.
- Frisby, J. P., Stone, J. V. (2010). *Seeing: The computational approach to biological vision*. MIT Press.
- Grove, O., Rajab, K., Piegl, et.al. (2011) From CT to NURBS: Contour Fitting with B-spline Curves. In *Computer-Aided Design and Applications*, V. 8(1), P. 3–21. doi: 10.3722/cadaps.2011.3-21.
- Jobson, D. J., Rahman, Z., Woodell, G. A. (1997) Properties and performance of a center/surround retinex. In *IEEE Transactions on Image Processing*, V. 6(3), P. 451–462. doi: 10.1109/83.557356
- Katz, B. (1982) Stephen William Kuffler, 24 August 1913 - 11 October 1980. In *Biographical memoirs of fellows of the Royal Society*, V. 28, P. 225–259. doi: 10.1098/rsbm.1982.0011.
- Kingman, J. (1993) *Poisson processes*. Clarendon Press.
- Land, E. H., McCann, J. (1971). Lightness and retinex theory. In *Journal of the Optical Society of America*, V. 61(1), P. 1–11. doi: 10.1364/JOSA.61.000001.
- Lisani, J.-L., Morel, J.-M., Petro, A.-B., Sbert, C. (2020). Analyzing center/surround retinex. In *Information sciences*, V. 512, P. 741–759. doi: 10.1016/j.ins.2019.10.009.
- Marr, D., Hildreth, E. (1980). Theory of edge detection. In *Proceedings of the Royal Society of London. Series B. Biological Sciences*, V. 207(1167), P. 187–217. doi: 10.1098/rspb.1980.0020.
- Masland, R. H. (2001) The fundamental plan of the retina. In *Nature Neuroscience*, V. 4(9), P. 877–886. doi: 10.1038/nn0901-877.
- Masland, R. (2020). *We know it when we see it: what the neurobiology of vision tells us about how we think*. Basic Books, New York.
- Murphy, K. P. (2012) *Machine Learning: A Probabilistic Perspective*, 1st ed., MIT Press, Cambridge.
- Robert, C. P., Casella, G. (2004). *Monte Carlo Statistical Methods*, 2nd ed. Springer, New York. doi: 10.1007/978-1-4757-4145-2.
- Streit, R. L. (2010). *Poisson Point Processes Imaging, Tracking, and Sensing*. Springer. doi: 10.1007/978-1-4419-6923-1.
- Vollmer, J., Mencl, R. and Müller, H. (1999) Improved Laplacian Smoothing of Noisy Surface Meshes. In *Computer graphics forum*, V. 18(3), P. 131–138. <https://doi.org/10.1111/1467-8659.00334>
- Wang, Y. K., Wang S.E. and Wu, P. H. (2023). Spike-Event Object Detection for Neuromorphic Vision. In *IEEE Access*, V. 11, P. 5215–5230. doi: 10.1109/ACCESS.2023.3236800.
- Young, G. A., Smith R. L. (2005). *Essentials of statistical inference*. Cambridge University Press, Cambridge.
- Zapp, S. J., Nitsche, S., Gollisch, T. (2022). Retinal receptive-field substructure: scaffolding for coding and computation. In *Trends Neurosci (Regular ed.)* V. 45(6), P. 430–445. doi: 10.1016/j.tins.2022.03.005.
- Zhang, F., and Bull, D. (2021). Measuring and managing picture quality, In *Intelligent Image and Video Compression 2nd ed*. Elsevier Science & Technology.
- Zhu S. C. and Wu, Y. N. (2023). *Computer Vision Statistical Models for Marr's Paradigm*, 1st ed. Cham: Springer.